PCP
PLANT & CELL PHYSIOLOGY

In Silico Simulation Modeling Reveals the Importance of the Casparian Strip for Efficient Silicon Uptake in Rice Roots

Gen Sakurai[1,*], Akiko Satake[2], Naoki Yamaji[3], Namiki Mitani-Ueno[3], Masayuki Yokozawa[4], François Gabriel Feugier[2] and Jian Feng Ma[3]

[1]Ecosystem Informatics Division, National Institute for Agro-Environmental Sciences, 3-1-3 Kannondai, Tsukuba, 305-8604 Japan
[2]Creative Research Initiative 'Sousei', Hokkaido University, N21, W10, Kita-ku, Sapporo, 001-0021 Japan
[3]Institute of Plant Science and Resources, Okayama University, 2-20-1 Chuo, Kurashiki, 710-0046 Japan
[4]Graduate School of Engineering, Shizuoka University, 3-5-1 Johoku Naka-ku, Hamamatsu, 432-8561 Japan
*Corresponding author: E-mail, sakuraigen@affrc.go.jp; Fax, +81-29-838-8224.
(Received August 20, 2014; Accepted January 27, 2015)

Silicon (Si) uptake by the roots is mediated by two different transporters, Lsi1 (passive) and Lsi2 (active), in rice (*Oryza sativa*). Both transporters are polarly localized in the plasma membranes of exodermal (outer) and endodermal (inner) cells with Casparian strips. However, it is unknown how rice is able to take up large amounts of Si compared with other plants, and why rice Si transporters have a characteristic cellular localization pattern. To answer these questions, we simulated Si uptake by rice roots by developing a mathematical model based on a simple diffusion equation that also accounts for active transport by Lsi2. In this model, we calibrated the model parameters using in vivo experimental data on the Si concentrations in the xylem sap and a Monte Carlo method. In our simulation experiments, we compared the Si uptake between roots with various transporter and Casparian strip locations and estimated the Si transport efficiency of roots with different localization patterns and quantities of the Lsi transporters. We found that the Si uptake by roots that lacked Casparian strips was lower than that of normal roots. This suggests that the double-layer structure of the Casparian strips is an important factor in the high Si uptake by rice. We also found that among various possible localization patterns, the most efficient one was that of the wild-type rice; this may explain the high Si uptake capacity of rice.

Keywords: Casparian strip • Polar localization • Nutrient uptake • Rice • Si • Transporters.

Abbreviations: Si, silicon; WT, wild type.

Introduction

Silicon (Si), the second most abundant element in soils, is beneficial for plant growth (Ma and Takahashi 2002). Si deposited in plant tissues enhances tolerance to abiotic and biotic stresses. For example, Si alleviates water stress, improves light interception characteristics by keeping the leaf blade erect and increases resistance to diseases, pests and lodging (Epstein 1994, Savant et al. 1997, Ma and Takahashi 2002).

Although all plant species contain Si, the Si content of above-ground tissues varies greatly among species (Hodson et al. 2005), ranging from 0.02% of dry mass to >10% (Ma and Takahashi 2002). Rice (*Oryza sativa*), a typical siliciphilous plant, can accumulate Si to >10% of its dry mass (Ma and Takahashi 2002). This high accumulation of Si is required for high and sustainable production of rice (Ma and Takahashi 2002, Tamai and Ma, 2008).

In rice roots, two main transporters are involved in Si uptake (Ma et al. 2006, Ma et al. 2007). The passive transporter OsLsi1 (hereafter, Lsi1) belongs to the aquaporin family and works based on diffusion along a concentration gradient, whereas the active transporter OsLsi2 (hereafter, Lsi2) is energy dependent, and mediates Si efflux from the cell to the apoplast associated with proton antiport (Ma et al. 2007, Ma et al. 2011). Both transporters are localized in the plasma membranes of the exodermal (outer) and endodermal (inner) cells, where Casparian strips are localized. The Casparian strips prevent the unimpeded movement of apoplastic substances into the interior tissues of the root, and also prevent backflow of ions and water (Enstone et al. 2003). Lsi1 is localized at the outer (distal) side of the cells, whereas Lsi2 is localized at the inner (proximal) side (Ma et al. 2006, Ma et al. 2007). Knockout of either Lsi1 or Lsi2 results in a significant decrease in Si accumulation (Ma et al. 2006, Ma et al. 2007), indicating that their co-operation is important for radial transport of Si from soil to the root stele.

Homologs of Lsi1 and Lsi2 were also identified in other plant species such as barley, maize and pumpkin. However, the cellular localization pattern differs depending on the species. HvLsi1 from barley and ZmLsi1 from maize are localized in epidermal, hypodermal and cortical cells, whereas CmLsi1 from pumpkin is found in all root cells (Chiba et al. 2009, Mitani et al. 2009b, Mitani et al. 2011). In barley and maize, HvLsi2 and ZmLsi2 do not show polar localization and are localized only in the root endodermis (Mitani et al. 2009a). These differences may be responsible for the different Si accumulation in rice and other species.

However, three main questions remain to be answered. (i) How can rice take up such large amounts of Si? (ii) Why do rice

Plant Cell Physiol. 56(4): 631–639 (2015) doi:10.1093/pcp/pcv017, Advance Access publication on 10 February 2015, available online at www.pcp.oxfordjournals.org

Si transporters have such a characteristic cellular localization pattern? (iii) What is the role of the Casparian strips in Si uptake? To address these questions, we performed simulation modeling (i.e. an in silico investigation). Simulation modeling has the following merits. (i) In silico, we can carry out experiments that would be difficult or impossible to conduct in vivo. For example, although it would be difficult to change the localization of the Si transporters in root cells in vivo, it is easy to change their localization and polarity in a simulation model. (ii) In silico, we can carry out a huge number of experiments with a large number of experimental settings if we have sufficient computational resources. For example, we can change the permeability of the cell membrane by changing the values of the model's parameters. (iii) In silico, we can visualize the processes involved in the target phenomenon. For example, we can reveal how Si is transported in the roots by visualizing the distribution of root Si concentrations at each time step.

In this study, we developed a mathematical model based on a simple diffusion equation that also accounts for the active transport by Lsi2 (Grieneisen et al. 2007). In this model, the dynamics of the Si uptake form, silicic acid [$Si(OH)_4$] , in root segments are simulated as a combination of diffusion and active transport processes from the root exodermis to the stele. The silicic acid is absorbed from the root epidermis by means of a diffusion process and transported inwards by Si transporters in the cell membranes. Our model differs from most previous simulation models, which combined diffusion of minerals between the cell membrane and the stele into one flux (e.g. Nye and Marriott 1969, Claassen et al. 1986, Roshani et al. 2009). In this study, we explicitly considered the spatial distribution of the transporters. Models that account for the spatial structure of the root have already been developed to study water and morphogen transport (Katou et al. 1987, Grieneisen et al. 2007, Grieneisen et al. 2012). Applying this methodology to the analysis of mineral transport allowed us to investigate the relationship between the transport and the root structure, including the localization and polarity of the mineral transporters. To ensure the validity of the model, we calibrated its parameters using in vivo experimental data from the Si concentration in the xylem sap of wild-type (WT) rice by applying a Monte Carlo method (Gelman et al. 2004).

Results

Model summary

In this model, we simulated the transport of Si from external solution into the xylem vessels. During its transport, Si passes through several cells by means of a diffusion process. Across the cell membranes, Si is transported out actively by Lsi2 and permeated passively by Lsi1, as well as by other factors that have not yet been identified (background leaking). Si cannot move across the apoplast region of Casparian strips (**Fig. 1**). By using this model, we can consider cell types with a range of transporter localizations (**Fig. 2**), including many that do not actually exist, and we can generate a range of root structures with a combination of the different cell types. We simulated the Si concentration in xylem sap at 60 min after placing the root in the Si solution (start of the simulation) for each of the various root structures, and used the results to answer the three study questions defined in the Introduction.

Model calibration

To calibrate the model, we assimilated the in vivo experimental data about the time series for the Si concentration in the xylem

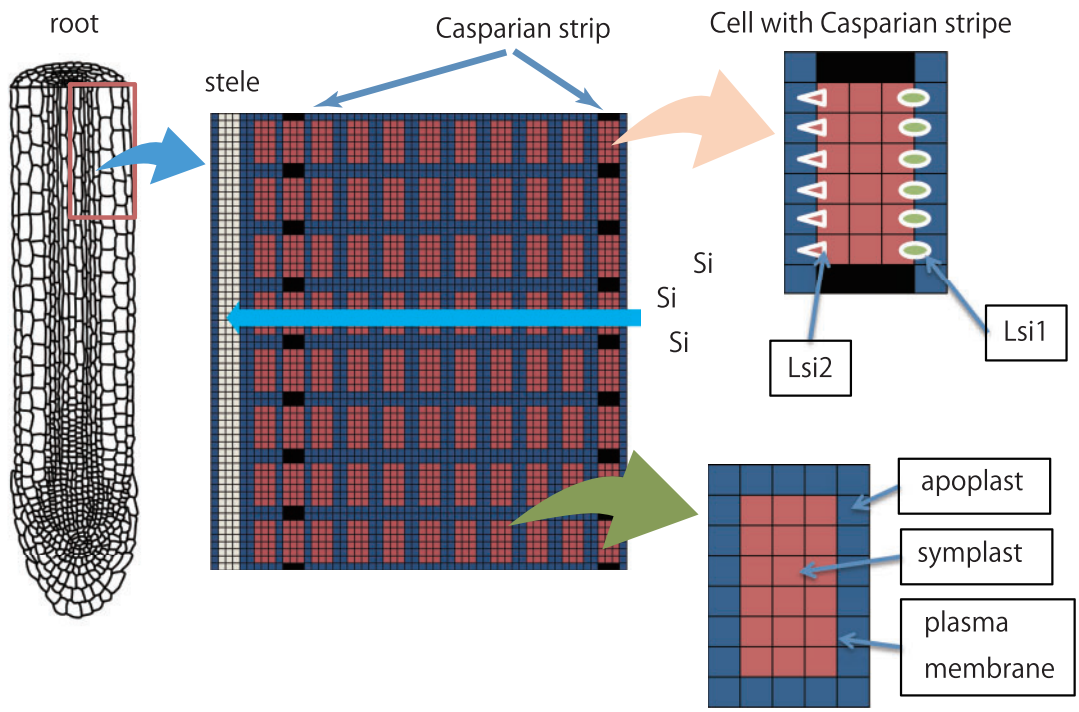

Fig. 1 Diagram of the root model. The dynamics of Si in the root segments were simulated from the root exodermis to the stele.

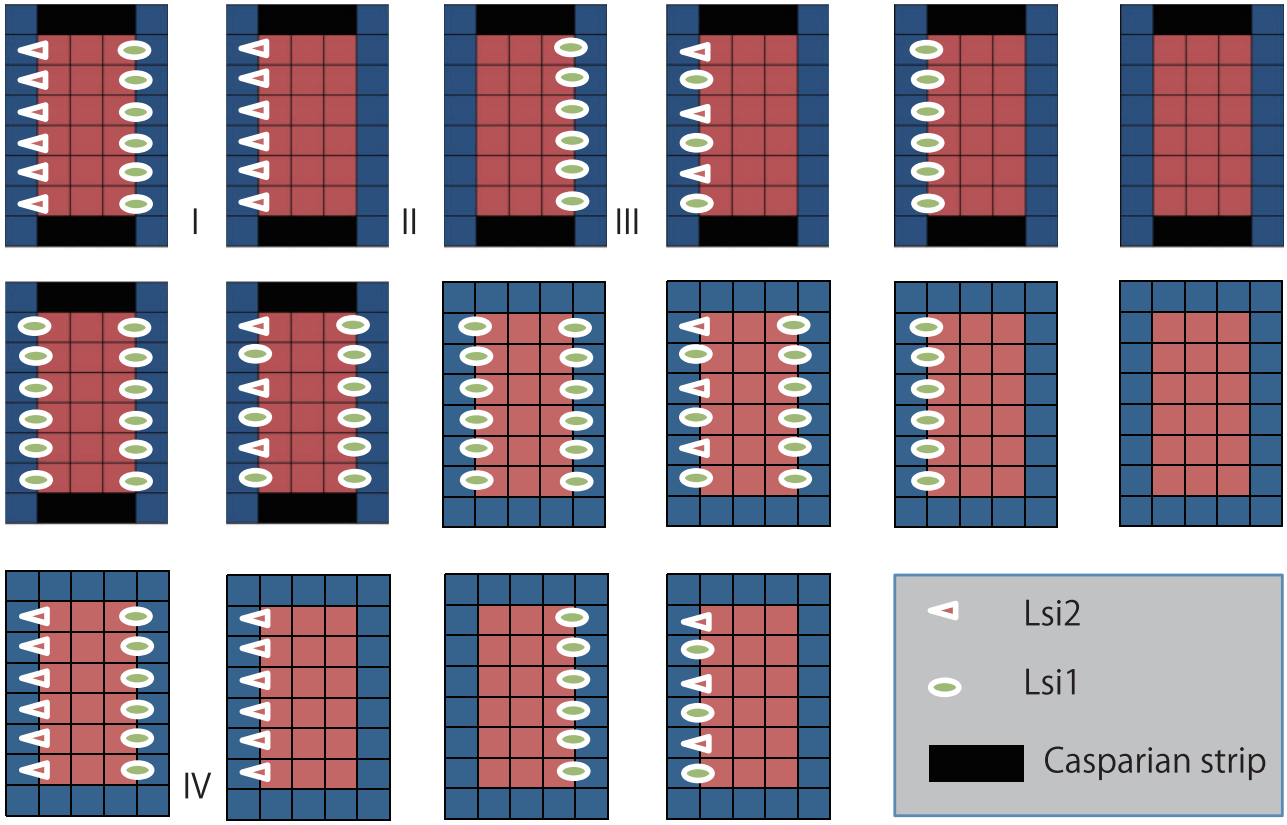

Fig. 2 The patterns used to define the localization of the transporters. For example, cell I indicates a cell of wild-type rice, cell II indicates a cell of the *lsi1* mutant and cell III indicates a cell of the *lsi2* mutant. We ignored the localization pattern in which Lsi2 was present at the outer side of the plasma membrane because this would obviously lead to low uptake.

sap into the mathematical model. To do so, we first determined the in vivo Si concentration in the xylem sap of WT rice. **Fig. 3** shows the time-dependent changes of the Si concentration after exposure to 1.0 mM Si solution. In the WT, the Si concentration in the xylem sap reached 5.0 mM at 5 min and continued to increase with time up to 25 min after exposure to Si, at which point the concentration reached a plateau (**Fig. 3**). Although the Si concentration appeared to decrease after 25 min, Yamaji and Ma (2011) showed that down-regulation of *Lsi2* was insignificant during the first day. Therefore, we did not consider the effect of down-regulation of Lsi expression in this model.

We estimated the probability distribution for three parameters of the model: the Lsi1 transporter permeability, the Lsi2 transporter activity and the permeability of the cell membrane (i.e. the background leaking). The average of the estimated probability distribution for the permeability of Lsi1 was $16.38 \pm 3.40\ \mu m\ s^{-1}$ (mean ± SD), the transport activity of Lsi2 was $4.48 \pm 0.26\ \mu m\ s^{-1}$ and the permeability of the cell membrane was $1.20 \pm 0.07\ \mu m\ s^{-1}$ (calculated by n = 300,000 Monte Carlo simulations). **Fig. 3** shows changes in the Si concentration over time calculated by the model using the estimated parameter set. The shaded area in **Fig. 3** is the 95% confidence interval. The root-mean-square error between the average simulated values and the observed values (simulated minus observed) for the WT was 3.29 mM. This result indicates that, although there is some uncertainty, our model can replicate the time course data of the Si concentration in the xylem sap of the WT.

Removal of the Casparian strips

To evaluate the role of the Casparian strips in Si transport, we compared the Si uptake abilities in root models with the following four settings. One was the normal setting (WT), in which the root has Casparian strips in both the exodermis and the endodermis, and the transporters are localized in the plasma membranes of the cells with the Casparian strips (hereafter, 'normal' roots). The others were model settings in which the Casparian strips of the endodermis, exodermis or both were 'removed', but the transporters were localized at the same position as in the normal roots (cell IV in **Fig. 2**): no Casparian strips in the endodermis (NC_{en}), in the exodermis (NC_{ex}) or in either tissue (NC_{en-ex}).

Fig. 4 shows the estimated Si concentration in the xylem sap for the normal, NC_{en}, NC_{ex} and NC_{en-ex} settings. The Si concentrations in the xylem sap decreased when the Casparian strips were removed. The estimated Si concentrations in the xylem sap 60 min after the roots were placed in the 1.0 mM Si solution were 12.69 ± 0.64 mM (mean ± SD) for the normal root, 5.06 ± 0.14 mM for the NC_{en} root 4.19 ± 0.12 mM for the NC_{ex} root and 1.35 ± 0.02 mM for the NC_{en-ex} root. These results confirm that the Casparian strips play an important role in Si transport in rice roots. Interestingly, the effects of the two strips were

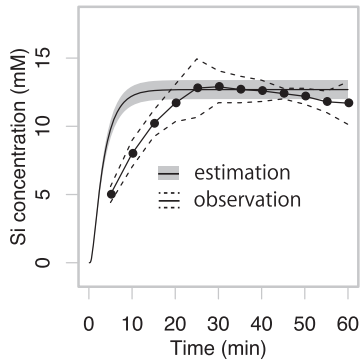

Fig. 3 Observed and simulated time course of the Si concentration in the xylem sap after the root was placed in the Si solution (1 mM) for wild-type rice. The dashed lines indicate the 95% confidence intervals for each plant type.

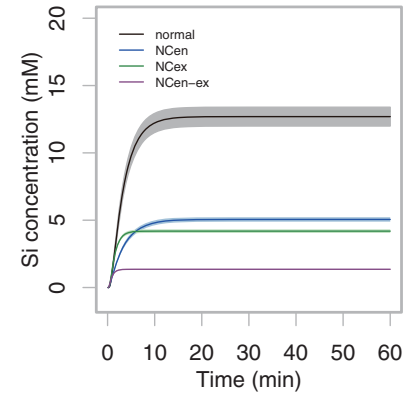

Fig. 4 Simulation of the time course of the Si concentration in the xylem sap after the root was placed in the Si solution (1 mM) for the normal rice and for rice with various modified Casparian strip patterns: no Casparian strip in the endodermis (NC_{en}), in the exodermis (NC_{ex}) or in both tissues (NC_{en-ex}). The shaded areas indicate 95% confidence intervals.

not simply additive. In comparison with the root with no Casparian strip, the Si concentration in the stele was increased by 3.70 and 2.83 mM by the addition of a Casparian strip in the exodermis or endodermis, respectively. However, the Si concentration was increased by 11.34 mM by the addition of Casparian strips in both the exodermis and the endodermis.

The average differences in the Si concentration between the stele and the cells between the endodermis and exodermis were 9.44 mM for the normal root and 0.69 mM for the NC_{en} root. The average differences between the cortex and the external solution (1.0 mM) were 2.25 mM for the normal root and 0.07 mM for the NC_{ex} root. This indicates that the Casparian strips play an important role in maintaining the Si gradient across both the endodermis and the exodermis.

Confirmation of the results under different model settings

We simulated Si transport under several different settings to examine the validity of the results. First, we simulated Si transport under a setting in which the Casparian strip was moved from the endodermis to an area between the epidermis and endodermis. Secondly, we simulated Si transport under a setting in which spatial resolution was changed: the value of d*x* was changed from 4.0 μm to 2.0 μm. Thirdly, we simulated Si transport under a setting in which the apoplast diffusion coefficient was lowered (to 500 $\mu m^2 s^{-1}$) because the default setting of the apoplast thickness may be larger than the actual apoplast thickness. We simulated Si transport with a low apoplast diffusion coefficient as an alternative to changing apoplast thickness. Fourthly, we simulated Si transport under a setting in which the root length was very long (40.0 mm). In all four cases, similar tendencies were observed: the Si concentrations in the stele were low when the Casparian strips were removed (**Supplementary Figs. S1–S4**).

Model validity and further confirmation of the results

We verified the model by comparing the estimated Si concentrations estimated for two mutants, the *lsi1* or *lsi2* mutants, with the actual concentrations measured in these mutants (**Supplementary Figs. S5**, **S6**). We predicted the time course of the Si concentration in the xylem sap under model settings in which Lsi1 permeability or Lsi2 activity was set to zero. The root-mean-square error values for the difference between the average simulated and observed values (simulated minus observed) were 2.88 mM for the *lsi1* mutant and 1.85 mM for the *lsi1* and *lsi2* mutant. The model replicated the large observed decrease in the Si concentration in the xylem sap in the mutants in comparison with the WT, even though the model was calibrated only by using WT data.

However, some discrepancies were observed between simulated and observed values, especially for the *lsi2* mutant. Interestingly, the observed Si concentration for the *lsi2* mutant exceeded 1.0 mM, the concentration of the Si solution. This observation suggests that another active transporter is present in the root; if the root has only Lsi2 as an active transporter, the concentration of the Si solution cannot be exceeded as suggested by the model.

Therefore, we conducted an additional experiment to confirm the importance of the Casparian strip for Si transport. We simulated a model that has an additional active transporter in the pericycle, and we compared the Si uptake of this root with that of a root lacking the Casparian strips. Again, the same tendency was observed: the Si concentration in the stele was low when the Casparian strips were removed (**Supplementary Fig. S7**).

Comparison of models with different arrangements of the transporters

We carried out simulation experiments in which Lsi1 and Lsi2 were localized in two other layers (the pericycle and cells between the endodermis and exodermis). In these simulations, we used the parameter values that had the highest likelihood among the 1,000 parameter sets (an Lsi1 transporter permeability of 19.92 $\mu m\, s^{-1}$, an Lsi2 transporter activity of 4.55 $\mu m\, s^{-1}$ and a cell membrane permeability of

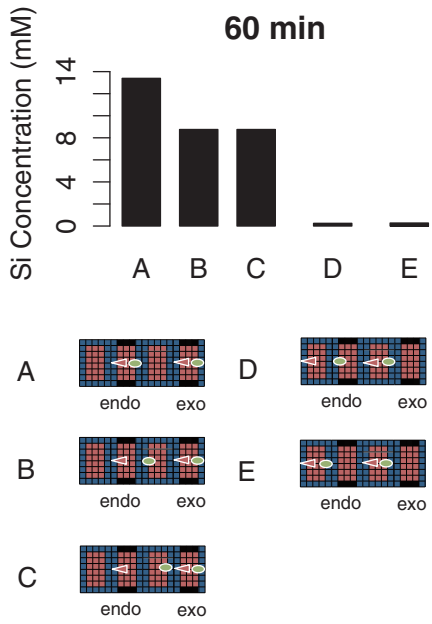

Fig. 5 Estimated Si concentrations in the xylem sap after 60 min in the models with the (A) highest, (B) second highest, (C) third highest and (D) lowest Si uptake among the 168 Lsi localization patterns of the transporters. In (E), the value was estimated by the model in which both transporters were present in the plasma membranes of cells in the pericycle and cortex.

1.21 μm s^{-1}). Because we assumed the root radius of 240 μm, the simulation model had eight cell layers between the endodermis and exodermis. In this experiment, we assumed that the transporters could exist at the pericycle layer and in the cell layer between the endodermis and exodermis. Therefore, we obtained a total of 168 possible localization patterns. (We excluded the localization pattern in which Lsi2 was present at the outer side of the plasma membrane because Lsi2 is an active efflux transporter from the symplast to the apoplast, and this would obviously lead to low uptake.)

Fig. 5 shows the estimated Si concentrations after 60 min in the models with the highest (**Fig. 5A**), second highest (**Fig. 5B**), third highest (**Fig. 5C**) and lowest (**Fig. 5D**) Si uptake among the 168 Lsi localization patterns and in the model in which both transporters were present at the plasma membrane of the cells in the pericycle and the cells between the endodermis and exodermis (**Fig. 5E**). The model with the highest Si uptake had the same localization pattern as in the normal root (13.39 mM at 60 min). The three models with the highest Si uptake had Lsi1 and Lsi2 transporters in the cells with Casparian strips in the exodermis (**Fig. 5A–C**). On the other hand, when the transporters were not localized in the cell with the Casparian strips, the Si uptake decreased greatly (**Fig. 5D, E**). These results also indicate the importance of the Casparian strips, and particularly that in the exodermis, for Si uptake.

Optimal investment in Si transporters and optimal localization

We compared the Si uptake among multiple model settings with different amounts of the Lsi1 and Lsi2 transporters and different localizations. In this study, we defined the Si transport efficiency as the Si concentration at 60 min divided by the number of layers in which the Si transporters were present. The resulting number of patterns totaled 1,296. We excluded the localization pattern in which Lsi2 was present at the outer side of the plasma membrane; we also excluded the pattern in which Lsi1 and Lsi2 coexisted in the same membrane because this would obviously lead to low transport efficiency. Because Lsi1 and Lsi2 should not have equal cost, we also evaluated the transport efficiencies with various relative costs of Lsi2 to Lsi1 (α).

Fig. 6a shows the relationship between the investment pattern and the relative transport efficiency at 60 min. The most efficient localization pattern for each investment pattern is shown. The most efficient investment and localization pattern after 60 min was that of the normal root, in which Lsi2 and Lsi1 were present at the inner and (outer) sides of the cells (respectively) in the inner and outer Casparian strips.

Fig. 6b–e show the relative transport efficiencies at 60 min when the relative investments in Lsi2 to Lsi1 (α) changed. In this figure, the values of α indicate the ratio of the cost of Lsi2 to the cost of Lsi1. For example, if $\alpha = 0.5$, the cost of Lsi2 is half that of Lsi1. When α is >0.5, the patterns with the most efficient uptake were the same as the most efficient patterns with $\alpha = 1.0$ at 60 min. When α is <0.5, the most efficient pattern changed slightly: the patterns with decreased investment in Lsi1 were most efficient. However, under all conditions, the most efficient patterns had Casparian strips with Lsi2 at the outer sides (**Fig. 6**).

Discussion

The role of the Casparian strips

The experiment in which the Casparian strips were removed from the endodermis and exodermis indicated that these strips play an important role in Si transport. One possible mechanism for enhanced Si transport in roots with two Casparian strips may be that the strips prevent backflow of Si from the stele. The Si gradients across the exodermis and endodermis were larger when the Casparian strips existed (see the Results).

The effects of the two strips were not simply additive. This was likely to have been the difference in the activity of the Lsi2 transporters in the endodermis. If the Si concentration in the cells between the endodermis and exodermis is roughly doubled, the transport ability of Lsi2 in the endodermis is also doubled. Metaphorically speaking, the Casparian strips in the exodermis are comparable with the first blade of a two-blade razor, and the Casparian strips in the endodermis represent the second blade. Because the first blade of the razor raises the beard hairs, the second blade can cut them more easily. By analogy, when the Casparian strips in the exodermis increase the Si concentration in the cells between the exodermis and endodermis, Lsi2 in the endodermis can more easily transport Si into the stele. This mechanism would result in a non-additive effect of the strips in the exodermis and endodermis on the Si concentration in the stele.

Casparian strips are formed by the accumulation of lignin and suberin in the primary cell wall (Schreiber 2010).

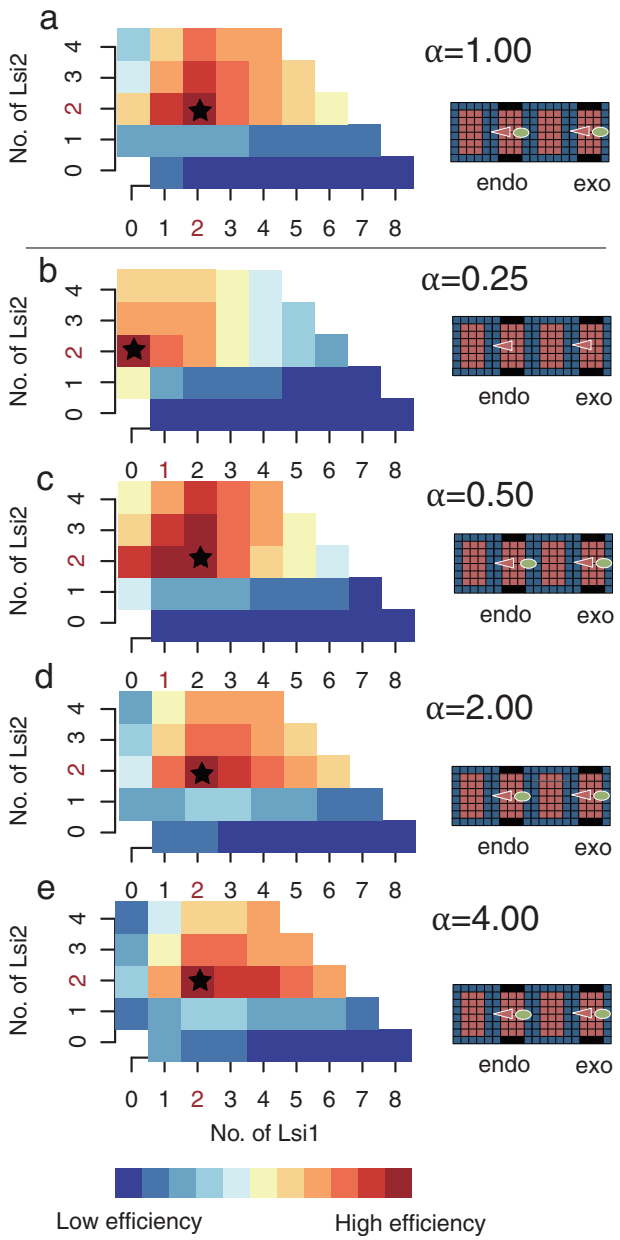

Fig. 6 Estimated transport efficiencies for multiple values of α based on the Si concentration at 60 min. The asterisk indicates the most efficient Lsi1 and Lsi2 investment pattern for each α value. There are multiple localization patterns of the transporters for each investment pattern. Therefore, the transport efficiency of the most effective localization pattern is shown for each investment pattern.

Many studies have investigated the physiological role of the Casparian strips (e.g. Enstone et al. 2003). The major role of the Casparian strips is to block the backflow of water, thereby maintaining high root pressure, which helps water movement upward (Steudle 1994). The other role that a Casparian strip plays is to block the diffusion of apoplastic substances across the strip, thereby allowing the endodermis and exodermis to act as ion filters (Ma and Peterson 2003). This also appears to be true for Si. However, the present results suggest an important role for Casparian strips in addition to their previously known functions. It is possible that plant species have evolved Casparian strips to block backflow of water, to select which minerals are taken up and to enhance the plant's ability to take up these minerals.

The most effective localization and polarity of the Si transporters

The most effective localization pattern for the transporters was with Lsi2 at the inner side of the cells in the Casparian strips and Lsi1 at the outer side when both are present at levels similar to those in the WT (**Fig. 5A**). If the Lsi transporters were localized in the cells without Casparian strips, the estimated Si concentrations in the xylem sap at 60 min after the root was placed in the Si solution were <2% of the levels obtained with the normal localization (**Fig. 5E**). This indicates that the Si transporters can work effectively only when they exist in the cells with the Casparian strips, and emphasizes the importance of the Casparian strips for Si transport.

Optimal investment and localization pattern for the transporters

In the above analysis, we determined the most effective localization pattern when the amount of investment in each transporter was fixed. However, the 'optimal' pattern represents a compromise between the costs of producing these transporters and the benefits of the resulting pattern. In this study, we also investigated the optimal amounts of investment in the transporters and their optimal localization pattern by evaluating the most effective localization patterns when the numbers of molecules of each transporter were not fixed. In addition, we analyzed the effects of the relative costs of Lsi2 to Lsi1, as represented by the α value, on the estimated optimal patterns.

When α is ≥1 (the relative cost of the expression of Lsi2 was higher than that of Lsi1), the most effective investment and localization patterns had Lsi2 at the inner side and Lsi1 at the outer side of the cells with Casparian strips at 60 min after the root was placed into the Si solution (**Fig. 5a, d, e**). This result was also obtained even at α ≥0.5, which indicated that the relative cost of *Lsi2* expression was higher than half of that of *Lsi1* expression. On the other hand, at α <0.5, the most effective pattern changed slightly; it had no Lsi1 transporters in the Casparian strips in the endodermis (**Fig. 6b**). However, the most important point is that the cost of utilizing Lsi2 should be higher than that of utilizing Lsi1 because transport of Si by Lsi2 is driven by a proton gradient that requires energy to be created, whereas Lsi1 is a passive transporter (Ma et al. 2007). The Lsi2 type of transport should require large amounts of energy for the maintenance and activity of the transporters. Therefore, if the benefit of the Si transport is defined as the quantity of Si uptake, the optimal strategy for Lsi production and localization would be the same as in the normal root, which represents the pattern in WT rice root.

Validity of the model

One of the important points of this study is that some of the model parameters were calibrated using in vivo experimental

data and a Monte Carlo method. Through this procedure, we can estimate the Si concentration in the xylem sap within reasonable bounds and we can discuss the results quantitatively.

One drawback of this study may be that we did not consider the flux of Si from the exodermis to the endodermis as a function of the magnitude of the water flow. However, a previous study suggested that the root hairs do not play an important role in Si uptake (Ma et al. 2001). This indirectly suggests that the amount of water flow does not greatly affect Si uptake, because, if root hairs do not exist, the uptake of water should decrease.

Another criticism of this study may be that the model does not consider the plasmodesmata. Plasmodesmata may increase symplast permeability for Si. Although we estimated the permeability of the membrane (background leakage) in this study, the membrane permeability allows for fluxes to arise due to concentration differences between apoplastic and cytosolic concentrations. On the other hand, the plasmodesmata allow fluxes to arise due to the concentration differences between cytosols. In this study, these passive diffusive processes directly between cells are not considered. We consider the refinement of the model as a future task.

A third criticism relates to an inconsistency between the predicted Si concentration in *lsi1* and *lsi2* mutants compared with the observed values. The calibrated model predicted a lower Si concentration for the *lsi2* mutant than for the *lsi1* mutant. On the other hand, the observed Si concentration was lower in the *lsi1* mutant than in the *lsi2* mutant. One possible explanation may be that as yet unidentified active transport mechanisms other than Lsi2 exist, for example at pericycle cells. This may represent an important problem to be solved in future research. However, our additional analysis revealed that the effect of the Casparian strips was retained even when a set of an additional active transporter and a passive transporter were present in pericycle cells (**Supplementary Fig. S7**). Therefore, we believe that our conclusion would still be valid even if transporters other than Lsi1 and Lsi2 are found. However, co-ordinated experimental and modeling studies are necessary to solve the inconsistency in **Supplementary Figs. S5** and **S6** in future studies.

Materials and Methods

Plant materials and xylem sap collection

Seeds of WT rice (*Oryza sativa* L. cv. 'Koshihikari') and two mutants (*lsi1* and *lsi2*) were soaked in water overnight at 25°C in the dark. The seeds were then transferred to a net that floated on a 0.5 mM $CaCl_2$ solution in a plastic container. On day 7, the seedlings were transferred to a 3.5 liter plastic pot containing half-strength Kimura B solution (Ma et al. 2001). The pH of this solution was 5.6, and the nutrient solution was renewed every 2 d.

For xylem sap collection, the seedlings (1 month old) were exposed to a solution containing 1.0 mM Si as silicic acid. Silicic acid was prepared by passing potassium silicate through a cation-exchange resin (Amberlite IR-120B, H^+ form; Organo) (Ma et al. 2001). At different time points indicated in **Fig. 3**, the shoots were decapitated with a razor at 1 cm above the roots, and the xylem sap was collected with a micropipette for 5 min. Three replicates were made at each time. The Si concentration in the xylem sap was determined as described previously (Ma et al. 2002).

Model description

Si is taken up by roots in the form of silicic acid (Mitani et al. 2005); then, it is translocated to the shoot in the form of monomeric silicic acid and deposited on the cell walls as amorphous silica (Yoshida 1965). In this study, we modeled the transfer of Si from outside of the root to the xylem.

Nutrients and other soluble substances move into the roots by diffusion and by mass flow induced by the transpiration stream (Nye and Marriott 1969). We simulated the transfer of Si in the roots using a diffusion equation on a two-dimensional grid, each grid point representing 4×4 μm (Grieneisen et al. 2007), and we calculated the transfer using a two-dimensional finite difference method (explicit). In our model, we only considered the transfer of Si within a small region of a root (**Fig. 1**). We assumed that each cell had 5×8 grids, respectively, in which the outermost grids were in the apoplast region (**Fig. 1**).

Most previous simulation models of mineral uptake have mathematically combined diffusion and the permeability of cell membranes to minerals into a single flux (e.g. Nye and Marriott 1969, Claassen et al. 1986, Roshani et al. 2009). In contrast, we accounted for the spatial structure of the cells in the present model (Grieneisen et al. 2007), which lets us evaluate the effects of the localization and polarity of the transporters on Si transport into the xylem sap. At the intracellular (symplast) and cell wall (apoplast) sites, Si diffuses freely at a rate determined by specific diffusion coefficients as follows:

$$\frac{\partial C}{\partial t} = D\left(\frac{\partial^2 C}{\partial z^2} + \frac{\partial^2 C}{\partial r^2}\right) \quad (1)$$

where C is the Si concentration (mM), t is time (s), D is the diffusion coefficient ($\mu m^2 s^{-1}$), z is the vertical co-ordinate (along the length of the root; μm) and r is the horizontal co-ordinate (in the radial direction; μm). We set the value of D to 1,000 $\mu m^2 s^{-1}$. At the xylem site, Si moves toward the above-ground part of the plant according to an advection–diffusion equation:

$$\frac{\partial C}{\partial t} = D\left(\frac{\partial^2 C}{\partial z^2} + \frac{\partial^2 C}{\partial r^2}\right) + u(r)\frac{\partial C}{\partial z} \quad (2)$$

where C is the Si concentration (mM), t is time (s), D is a diffusion coefficient ($\mu m^2 s^{-1}$), z is the vertical co-ordinate (along the length of the root; μm), r is the horizontal co-ordinate (in the radial direction; μm) and $u(r)$ is the velocity of the xylem sap ($\mu m\, s^{-1}$).

We considered two cell types in our analysis (with and without Casparian strips), and we considered various transporter locations (**Fig. 2**). In a cell without Casparian strips, the intracellular space is surrounded by the apoplast region. In a cell with Casparian strips, the intracellular space is also surrounded by the apoplast region, but Si cannot diffuse through the apoplastic region containing the Casparian strips.

Si moves through the cell membrane following three pathways. First, Si can move between the symplast and apoplast through Lsi1 (**Fig. 1**), driven by a concentration difference between the two sites. Secondly, Si can be actively transported out from the symplast to the apoplast through the active efflux transporter, Lsi2, at a rate that depends on the Si concentration in the symplast (Grieneisen et al. 2007). Thirdly, we assumed low permeability of the cell membrane itself (not via Lsi transporters: background leaking). In summary, the Si flux across the plasma membrane is described by the following equation:

$$\vec{J}_{mem} = -(\rho_{Lsil}\vec{n})(C_{in} - C_{out}) - (\rho_{Lsil}\vec{n})C_{in} - (\rho_m\vec{n})(C_{in} - C_{out}) \quad (3)$$

where $\vec{J}_{mem}$ is Si flux across the plasma membrane (mM $\mu m\, s^{-1}$); C_{in} and C_{out} are the Si concentrations in the symplast and apoplast, respectively, at the grid points immediately adjacent to the plasma membrane; ρ_m is the permeability of the plasma membrane ($\mu m\, s^{-1}$); ρ_{Lsi1} is the permeability of the Lsi1 transporter ($\mu m\, s^{-1}$); ρ_{Lsi2} is the transport activity of the Lsi2 transporter ($\mu m\, s^{-1}$); and $\vec{n}$ is the inward- (from the apoplast to the symplast) directed unit vector that is perpendicular to the plasma membrane (Grieneisen et al. 2007). Therefore, the dynamics for Si in the grid points that are immediately adjacent to the plasma membrane become:

$$\frac{\partial C}{\partial t} = D\left(\frac{\partial^2 C}{\partial z^2} + \frac{\partial^2 C}{\partial r^2}\right) + \frac{\vec{J}_{mem,z}}{\partial z} + \frac{\vec{J}_{mem,r}}{\partial r} \quad (4)$$

where $\vec{J}_{mem,z}$ is Si flux across the plasma membrane in the z direction and $\vec{J}_{mem,r}$ is Si flux across the plasma membrane in the r direction. We had to consider the

cylindrical shape of the root; therefore, we corrected the diffusion equation for the apoplast and symplast for the *r*-axis direction in the actual simulation as below:

$$\frac{\partial C}{\partial t} = D\left[\frac{\partial^2 C}{\partial z^2} + \frac{1\partial}{r\partial r}\left(r\frac{\partial C}{\partial r}\right)\right] + \frac{\vec{J}_{mem,z}}{\partial z} + \frac{1\partial}{r\partial r}(r\vec{J}_{mem,r}) \quad (5)$$

For the normal setting (assuming WT), Lsi1 and Lsi2 are localized only in the cell membrane of the Casparian strip cells, and exhibit polarity (i.e. the transporters are localized on specific sides of the membrane), and Casparian strips exist at both the endodermis and the exodermis.

The boundary conditions at the upper limit and lower limit of the root were Neumann boundary conditions (with the fluxes across the boundary set to zero). The Si concentration outside the root was fixed at 1.0 mM in all experiments. In all the simulation experiments, we arbitrarily set the root length to 64 μm (two cells) because our preliminary analysis suggests that the root length does not greatly affect the Si concentration in the xylem sap in this model (see **Supplementary Table S1**). We set the root width to 240 μm. Although we also assumed a specific value for the flow of the xylem sap in this model, the strength of the flow did not greatly affect the Si concentration in the xylem sap in our preliminary analysis (see **Supplementary Table S2**). Therefore, we set the strength of the flow as $u(z,r) = 0$ in all experiments.

Model calibration

We calculated 1,000 simulations with different parameter sets of the model. Then, we calculated the likelihood for each simulation member in accordance with the in vivo experimental data. Finally, we resampled the parameter sets based on their likelihoods. Using the resampled 100 parameter sets, we conducted the simulation experiments.

In the calibration procedure, we estimated the posterior distribution of the parameters relevant to the permeability of the Lsi1 transporter (ρ_{Lsi1}), the permeability of the plasma membrane (ρ_m) and the Lsi2 transporter activity (ρ_{Lsi2}). The value of *D* was fixed at 1,000.0 $\mu m^2 s^{-1}$, although Grieneisen et al. (2007) chose a value of 600.0 $\mu m^2 s^{-1}$ for auxin [because the molecular size of $Si(OH)_4$ is smaller than that of auxin]. This value was arbitrary because we found no information about the actual diffusion coefficient for Si in the symplast and apoplast. However, we believe that this choice did not affect the qualitative conclusions drawn from our study, because the difference between the real and model values should have been compensated for by the calibration procedure used to determine the values of the other parameters.

First, we generated 1,000 parameter sets from uniform distributions of values from 0.0 to 20.0 for ρ_{lsi1}, from 0.0 to 2.0 for ρ_m and from 0.0 to 5.0 for ρ_{Lsi2}. Then, we simulated the model for each parameter set. We calculated the likelihood for each parameter set as follows;

$$L(\theta|Data) = \Pi\frac{1}{\sqrt{2\pi\sigma^2}}\exp\left(-\frac{(C_{est,j}(\theta) - C_{obs,j})^2}{2\sigma^2}\right) \quad (6)$$

where *L* is the likelihood of parameter set θ under the observed data set *Data*, σ is the standard deviation of the error distribution, $C_{est,i}(\theta)$ is the simulated Si concentration in the xylem sap at time *i* with parameter set θ, and $C_{obs,i}$ is the observed Si concentration at time *i*. We resampled 300,000 parameter sets allowing replacement based on the calculated likelihood. In this procedure, the value of σ (the estimation error of the model) was also randomly selected for each parameter set because we did not have any information about σ. From these resampled parameter sets, we estimated the means and standard deviation of the parameters. For the simulation experiment, we used only 100 parameter sets that were randomly selected from the resampled parameter sets.

Transport efficiency

We defined the transport efficiency as follows;

$$E = \frac{C_i}{n_{lsi1} + \alpha n_{lsi2}} \quad (7)$$

where *E* is the transport efficiency, C_i is the Si concentration (mM) in the xylem sap at time *i*, n_{lsi1} is the number of layers in which Lsi1s are expressed, n_{lsi2} is the number of layers in which Lsi2s are expressed and α is the relative cost of Lsi2 to Lsi1 (e.g. a low value of α means that the cost of Lsi2 is lower than that of Lsi1). To determine the optimal transport efficiency, we set the number of cells in the cortex to only one cell. Therefore, the total number of cells was four, except for the cells that comprised the xylem, in a horizontal direction. This means that the maximum value for both n_{lsi1} and n_{lsi2} was eight. However, we excluded the localization pattern in which Lsi2 was present at the outer side of the plasma membrane. Therefore, the maximum value for n_{lsi2} was four.

Supplementary data

Supplementary data are available at PCP online.

Funding

This study was supported by the Ministry of Education, Culture, Sports, Science and Technology of Japan (MEXT) [Grants-in-Aid for Scientific Research in Innovative Areas (grant No. 70452737 to G.S., No. 22119009 to A.S. and No. 22119002 to J.F.M.) and as part of a Joint Research Program implemented at the Institute of Plant Science and Resources, Okayama University in Japan]. The funders had no role in the study design, data collection and analysis, decision to publish or preparation of the manuscript. Computations were carried out on a cluster system at the Agriculture, Forestry and Fisheries Research Information Technology Center for Agriculture, Forestry and Fisheries Research, Ministry of Agriculture, Forestry and Fisheries, Japan.

Acknowledgments

We thank Mr. Kentaro Ohigashi (NIAES) for helpful advice on the model description.

Disclosures

The authors declare no conflicts of interest.

References

Chiba, Y., Mitani, N., Yamaji, N. and Ma, J.F. (2009) HvLsi1 is a silicon influx transporter in barley. *Plant J.* 57: 810–818.

Claassen, N., Syring, K.M. and Jungk, A. (1986) Verification of mathematical model by simulating potassium uptake from soil. *Plant Soil* 95: 209–220.

Enstone, D.E., Peterson, C.A. and Ma, F. (2003) Root endodermis and exodermis: structure, function, and responses to the environment. *J. Plant Growth Regul.* 21: 335–351.

Epstein, E. (1994) The anomaly of silicon in plant biology. *Proc. Natl Acad. Sci. USA* 91: 11–17.

Gelman, A., Carlin, J.B., Stern, H.S. and Rubin, D.B. (2004) Bayesian Data Analysis, 2nd edn. Chapman Hall/CRC, New York.

Grieneisen, V.A., Scheres, B., Hogeweg, P. and Marée, A.F.M. (2012) Morphogengineering roots: comparing mechanisms of morphogen gradient formation. *BMC Syst. Biol.* 6: 37.

Grieneisen, V.A., Xu, J., Marée, A.F.M., Hogeweg, P. and Scheres, B. (2007) Auxin transport is sufficient to generate a maximum and gradient guiding root growth. *Nature* 449: 1008–1013.

Hodson, M.J., White, P.J., Mead, A. and Broadley, M.R. (2005) Phylogenetic variation in the silicon composition of plants. *Ann. Bot.* 96: 1027–1046.

Katou, K., Taura, T. and Furomoto, M. (1987) A model for transport in the stele of plant roots. *Protoplasma* 140: 123–132.

Ma, F. and Peterson, C.A. (2003) Current insights into the development, structure, and chemistry of the endodermis and exodermis of roots. *Can. J. Bot.* 81: 405–421.

Ma, J.F., Higashitani, A., Sato, K. and Takeda, K. (2003) Genotypic variation in silicon concentration of barley grain. *Plant Soil* 249: 383–387.

Ma, J.F., Goto, S., Tamai, K. and Ichii, M. (2001) Role of root hairs and lateral roots in silicon uptake by rice. *Plant Physiol.* 127: 1773–1780.

Ma, J.F. and Takahashi, E. (2002) Soil, Fertilizer, and Plant Silicon Research in Japan. Elsevier, The Netherlands.

Ma, J.F., Tamai, K., Yamaji, N., Mitani, N., Konishi, S., Katsuhara, M. et al. (2006) A silicon transporter in rice. *Nature* 440: 688–691.

Ma, J.F., Yamaji, N., Mitani, N., Tamai, K., Konishi, S., Fujiwara, T. et al. (2007) An efflux transporter of silicon in rice. *Nature* 448: 209–213.

Ma, J.F., Yamaji, N. and Mitani-Ueno, N. (2011) Transport of silicon from roots to panicles in plants. *Proc. Jpn. Acad. Ser. B* 87: 377–385.

Mitani, N., Chiba, Y., Yamaji, N. and Ma, J.F. (2009a) Identification and characterization of maize and barley Lsi2-like silicon efflux transporters reveals a distinct silicon uptake system from that in rice. *Plant Cell* 21: 2133–2142.

Mitani, N., Ma, J.F. and Iwashita, T. (2005) Identification of the silicon form in xylem sap of rice (*Oryza sativa* L.). *Plant Cell Physiol.* 46: 279–283.

Mitani, N., Yamaji, N., Ago, Y., Iwasaki, K. and Ma, J.F. (2011) Isolation and functional characterization of an influx silicon transporter in two pumpkin cultivars contrasting in silicon accumulation. *Plant J.* 66: 231–240.

Mitani, N., Yamaji, N. and Ma, J.F. (2009b) Identification of maize silicon influx transporters. *Plant Cell Physiol.* 50: 5–12.

Nye, P.H. and Marriott, F.H.C. (1969) A theoretical study of the distribution of substances around roots resulting from simultaneous diffusion and mass flow. *Plant Soil* 3: 459–172.

Roshani, G.A., Narayanasamy, G. and Datta, S.C. (2009) Modelling potassium, uptake by wheat. *Int. J. Plant Prod.* 3: 55–68.

Savant, N.K., Snyder, G.H. and Datnoff, L.E. (1997) Silicon management and sustainable rice production. *Adv. Agron.* 58: 151–199.

Schreiber, L. (2010) Transport barriers made of cutin, suberin and associated waxes. *Trends Plant Sci.* 15: 1360–1385.

Steudle, E. (1994) Water transport across roots. *Plant Soil* 167: 79–90.

Tamai, K. and Ma, J.F. (2008) Reexamination of silicon effects on rice growth and production under field conditions using a low silicon mutant. *Plant Soil* 307: 21–27.

Yamaji, N. and Ma, J.F. (2011) Futher characterization of a rice silicon efflux transporter, Lsi2. *Soil Sci. Plant Nutr.* 57: 259–264.

Yoshida, S. (1965) Chemical aspects of the role of silicon in physiology of the rice plant. *Bull. Natl Inst. Agric. Sci. B* 15: 1–58.